

Figure 2: **Evaluating Rationales via RLC/Sim.** Given task input \mathbf{x}_i and the task LM’s predicted label \hat{y}_i , we can measure rationale (\mathbf{r}_i) quality based on *rationale-label consistency* (RLC). RLC is implemented using *simulatability* (sim), *i.e.*, how accurately a simulator (*i.e.*, LM or human observer) predicts \hat{y}_i using both task \mathbf{x}_i and \mathbf{r}_i as input, compared to using only \mathbf{x}_i .

ing the task LM’s predicted label (Doshi-Velez and Kim, 2017; Hase and Bansal, 2020)? It follows that sim (*i.e.*, RLC) at least partially reflects how aligned the rationale is with the simulator’s reasoning process for reaching the predicted label. Therefore, as the simulator can be an LM or human (Hase et al., 2020), RLC can be seen as a prerequisite for key rationale desiderata like *faithfulness* (alignment with LM’s reasoning) (Jacovi and Goldberg, 2020) and *plausibility* (alignment with humans’ reasoning) (DeYoung et al., 2019). Though RLC may not fully capture these desiderata, it may still provide useful signal about them. However, there is no standard protocol for evaluating RLC metrics’ reliability, so their effectiveness remains unclear.

In light of this, we propose **Free-Text Rationale-Label Consistency Meta-Evaluation (FRAME)**, a framework for evaluating RLC metrics for free-text rationales. FRAME is based on three axioms: (1) good metrics should yield highest scores for *reference rationales*, which maximize RLC by construction; (2) good metrics should be appropriately sensitive to semantic perturbation of rationales; and (3) good metrics should be robust to variation in the task LM’s task performance. For (1), we simply define the reference rationale as the task LM’s predicted label. This provides a powerful invariance

for analyzing the quality of free-text rationales, whose unconstrained nature typically makes such analysis difficult. For (2), we test if the metric responds appropriately to equivalent (should not change meaning) and contrastive (should change meaning) perturbations of reference rationales. For (3), we compute RLC as a function of the task LM’s task performance, by varying factors like the task LM’s number of train instances, number of noisy train instances, and capacity. We also separately compute RLC on correctly and incorrectly predicted test instances, to check if it is stable across these two subpopulations.

On three text classification datasets—e-SNLI, CoS-E v1.0, and CoS-E v1.11—we show that existing RLC metrics cannot satisfy all three FRAME axioms. Since they involve pretraining simulators on external corpora, existing RLC metrics struggle to isolate the rationale’s contribution to simulator accuracy from the pretraining knowledge’s, hence muddling the metric’s signal. Thus, we introduce a non-pretraining RLC metric, NP- \mathcal{GH} -PRED, to address this issue. For LM simulators, NP- \mathcal{GH} -PRED improves performance on (1) and (3) by an average of 41.7% and 42.9%, respectively, while performing competitively on (2) (Sec. 4.2). For human simulators, we conduct a user study of (1), with NP- \mathcal{GH} -PRED improving performance on (1) by 47.7% (Sec. 4.3). Based on these results, we discuss the inherent limitations of using RLC to measure free-text rationale quality (Sec. 6).

2 Free-Text Rationales

Let $\mathcal{F}_{\text{task}}$ denote a task LM for m -class text classification. For task instance i , let $\mathbf{x}_i = [x_i^t]_{t=1}^{n_x}$ be the n_x -token input sequence (*e.g.*, a sentence), y_i be the gold label, and \hat{y}_i be $\mathcal{F}_{\text{task}}$ ’s predicted label. Let $\hat{\mathbf{y}}_i = [\hat{y}_i^t]_{t=1}^{n_y}$ and $\hat{\mathbf{y}}_i = [\hat{y}_i^t]_{t=1}^{n_y}$ be token sequence representations of y_i and \hat{y}_i , respectively. A *free-text rationale* $\mathbf{r}_i = [r_i^t]_{t=1}^{n_r}$ is an n_r -token sequence that uses natural language to explain the reasoning process behind $\mathcal{F}_{\text{task}}$ predicting \hat{y}_i (Fig. 1-4).

2.1 Free-Text Rationale Generation

Unlike extractive rationales, which are constrained to scoring tokens in \mathbf{x}_i , free-text rationales can have arbitrary content, style, and length (*i.e.*, n_r) (Narang et al., 2020; Camburu et al., 2018). Free-text rationales can be generated via any means, but are typically generated by an explainer LM $\mathcal{F}_{\text{expl}}$. In general, we use \mathbf{r}_i to denote a free-text rationale

with no assumptions about its generation process, but we specifically denote $\mathcal{F}_{\text{expl}}$'s predicted rationale as $\hat{\mathbf{r}}_i$. While $\mathcal{F}_{\text{task}}$ and $\mathcal{F}_{\text{expl}}$ can be separate (Kumar and Talukdar, 2020; Rajani et al., 2019; Camburu et al., 2018), *self-rationalizing LMs* combine $\mathcal{F}_{\text{task}}$ and $\mathcal{F}_{\text{expl}}$ into a single LM \mathcal{F} , which jointly generates the task and rationale outputs (Narang et al., 2020; Lakhotia et al., 2020; Do et al., 2020; Liu et al., 2018) (Fig. 1). In particular, text-to-text self-rationalizing LMs (e.g., T5 (Raffel et al., 2019)) output an $(n_y + n_r)$ -token sequence $[\hat{\mathbf{y}}_i, \hat{\mathbf{r}}_i]$. Following recent works (Hase et al., 2020; Wiegrefe et al., 2021), we focus on T5-based self-rationalizing LMs as \mathcal{F} .

2.2 Free-Text Rationale Evaluation

Given \mathbf{x}_i and \mathcal{F} , existing free-text rationale metrics evaluate \mathbf{r}_i by measuring the consistency between \mathbf{r}_i and $\hat{\mathbf{y}}_i$, denoted as *rationale-label consistency* (RLC) or $\rho(\mathbf{r}_i, \hat{\mathbf{y}}_i, \mathbf{x}_i; \mathcal{F})$. ρ is computed via *simulatability* (sim), which measures how predictive \mathbf{r}_i is of $\hat{\mathbf{y}}_i$ (Doshi-Velez and Kim, 2017; Hase and Bansal, 2020). That is, how accurately does a *simulator* (i.e., observer) predict $\hat{\mathbf{y}}_i$ using both \mathbf{x}_i and \mathbf{r}_i as input, compared to using only \mathbf{x}_i ? It follows that sim (i.e., RLC) at least partially reflects how aligned \mathbf{r}_i is with the simulator's reasoning process for reaching $\hat{\mathbf{y}}_i$. Let Φ be a RLC metric and \mathcal{S} be a simulator. Then, $\Phi(\mathbf{r}_i, \hat{\mathbf{y}}_i, \mathbf{x}_i; \mathcal{F}, \mathcal{S}) = \mathbb{1}_{\mathcal{S}}(\hat{\mathbf{y}}_i | \mathbf{x}_i, \mathbf{r}_i) - \mathbb{1}_{\mathcal{S}}(\hat{\mathbf{y}}_i | \mathbf{x}_i)$, where $0 \leq \mathbb{1}_c(b | a) \leq 100$ is c 's accuracy in predicting b given a . $\mathbb{1}_{\mathcal{S}}(\hat{\mathbf{y}}_i | \mathbf{x}_i)$ and $\mathbb{1}_{\mathcal{S}}(\hat{\mathbf{y}}_i | \mathbf{x}_i, \mathbf{r}_i)$ are the *control* and *treatment* terms, respectively, with higher Φ indicating higher ρ (i.e., \mathbf{r}_i quality). The rationale desideratum (e.g., faithfulness, plausibility) addressed by Φ is determined by the choice of \mathcal{S} (e.g., LM, human). We discuss this below.

LM Simulators For faithfulness, we can set \mathcal{S} as another LM (Hase et al., 2020; Wiegrefe et al., 2021), such that Φ reflects \mathbf{r}_i 's alignment with the LM's reasoning process for reaching $\hat{\mathbf{y}}_i$. In doing so, prior works implicitly make two strong assumptions. First, they assume ρ is sufficiently informative about \mathcal{F} 's reasoning process w.r.t. \mathbf{r}_i , $\hat{\mathbf{y}}_i$, and \mathbf{x}_i . Although a rationale that maximizes ρ may not necessarily explain \mathcal{F} 's entire reasoning process, such a rationale may still provide useful signal about \mathcal{F} 's behavior. Second, despite them being different LMs, they assume \mathcal{S} 's reasoning process is sufficiently similar to \mathcal{F} 's w.r.t. the given task, such that \mathcal{S} 's behavior reflects \mathcal{F} 's. This is needed

because using \mathcal{F} as the simulator would trivially result in perfect $\hat{\mathbf{y}}_i$ prediction accuracy for the control term, rendering Φ meaningless.

In practice, it can be difficult for \mathcal{S} to jointly approximate the $P(\cdot | \mathbf{x}_i)$ and $P(\cdot | \mathbf{x}_i, \mathbf{r}_i)$ distributions. To address this issue, Wiegrefe et al. (2021) decomposes \mathcal{S} into two LMs: \mathcal{G} for $P(\cdot | \mathbf{x}_i)$ and \mathcal{H} for $P(\cdot | \mathbf{x}_i, \mathbf{r}_i)$. Meanwhile, Hase et al. (2020) trains \mathcal{S} to approximate both $P(\cdot | \mathbf{x}_i)$ and $P(\cdot | \mathbf{x}_i, \mathbf{r}_i)$ by randomly dropping out either \mathbf{x}_i or \mathbf{r}_i from the input during training. In this paper, we follow the first approach, since it enables us to use the same standard training process for all LMs. We call \mathcal{G} (Fig. 3) and \mathcal{H} (Fig. 4) the *control LM* and *treatment LM*, respectively. Then, Φ is computed as: $\Phi(\mathbf{r}_i, \hat{\mathbf{y}}_i, \mathbf{x}_i; \mathcal{F}, \mathcal{G}, \mathcal{H}) = \mathbb{1}_{\mathcal{H}}(\hat{\mathbf{y}}_i | \mathbf{x}_i, \mathbf{r}_i) - \mathbb{1}_{\mathcal{G}}(\hat{\mathbf{y}}_i | \mathbf{x}_i)$. Unless Φ is specifically not defined w.r.t. $\hat{\mathbf{y}}_i$, \mathbf{x}_i , \mathcal{F} , \mathcal{G} , and \mathcal{H} , we abbreviate $\Phi(\mathbf{r}_i, \hat{\mathbf{y}}_i, \mathbf{x}_i; \mathcal{F}, \mathcal{G}, \mathcal{H})$ as $\Phi(\mathbf{r}_i)$.

Human Simulators For plausibility, \mathcal{S} is a human, such that Φ reflects \mathbf{r}_i 's alignment with humans' reasoning process for reaching $\hat{\mathbf{y}}_i$ (Doshi-Velez and Kim, 2017; Hase and Bansal, 2020; Chan et al., 2022). Note that sim was originally defined in the context of plausibility (Doshi-Velez and Kim, 2017), before being adapted for faithfulness (Hase et al., 2020). Like in faithfulness, this implicitly assumes all humans share a sufficiently similar reasoning process w.r.t. the given task. We use the same \mathcal{S} for both $P(\cdot | \mathbf{x}_i, \mathbf{r}_i)$ and $P(\cdot | \mathbf{x}_i)$, since a human \mathcal{S} generally does not require fine-tuning.

Issues with RLC Metrics Intuitively, RLC metrics cannot fully capture faithfulness or plausibility, as RLC provides only a narrow view of LMs' or humans' reasoning processes. Also, we see that using RLC for this narrow faithfulness or plausibility evaluation still requires relatively strong assumptions. Since RLC is currently the only available tool for evaluating rationale quality, one may be inclined to use RLC metrics by default. However, there exists no protocol for evaluating RLC metrics themselves, so it is unclear how reliable they are.

3 FRAME

In Sec. 2.2, we defined Φ as a metric for evaluating rationale quality via RLC (i.e., ρ). Ideally, Φ should capture only ρ , without entangling other orthogonal information (e.g., \mathcal{F} 's task performance). While a number of Φ metrics have been proposed (Hase et al., 2020; Wiegrefe et al., 2021), there is no stan-

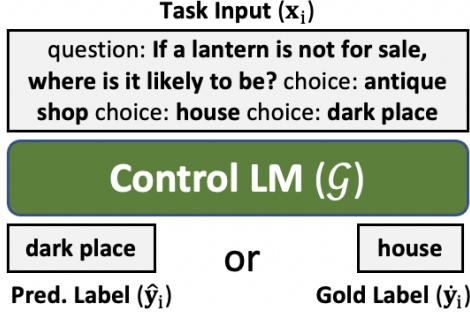


Figure 3: **Control LM**. Given task input x_i , the control LM (\mathcal{G}) is an LM simulator trained to generate either \mathcal{F} 's predicted label \hat{y}_i or the gold label \hat{y}_i .

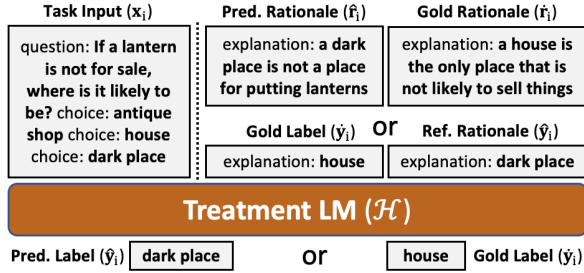


Figure 4: **Treatment LM**. Given task input x_i and some rationale (one of r_i , \hat{y}_i , \hat{r}_i , or \hat{y}_i), the treatment LM (\mathcal{H}) is an LM simulator trained to generate either \mathcal{F} 's predicted label \hat{y}_i or the gold label \hat{y}_i .

dard protocol for evaluating Φ , so it is unclear if such metrics are behaving as desired. Thus, we propose FRAME, a general framework for evaluating Φ . FRAME assesses Φ according to three axioms: (1) good metrics should yield highest scores for reference rationales, which maximize RLC by construction; (2) good metrics should be appropriately sensitive to semantic perturbation of rationales; and (3) good metrics should be robust to variation in the task LM's task performance. FRAME can be used to evaluate Φ w.r.t. both LM and human simulators. Still, in this work, we mainly focus on LM simulators, since they are fully automated. Sec. 3.1 introduces each axiom and its corresponding meta-metrics for Φ , Sec. 3.2 provides implementation details for each axiom's meta-metrics, and Sec. 3.3 describes all RLC metrics considered in the paper.

3.1 FRAME Axioms and Meta-Metrics

Axiom 1: Reference Rationale Upper Bound

In certain respects, the quality of r_i can be measured as $\rho(r_i, \hat{y}_i)$, the consistency between r_i and \hat{y}_i (Sec. 2.2). Intuitively, $\arg \max_{r_i} \rho(r_i, \hat{y}_i) = \hat{y}_i$, since \hat{y}_i should be maximally consistent with itself. It follows that Φ should yield a higher score for \hat{y}_i than for any other rationale, such that

$\arg \max_{r_i} \Phi(r_i) = \hat{y}_i$. We call \hat{y}_i the *reference rationale*, which serves as an upper bound for $\Phi(r_i)$. Given the high complexity of NLM reasoning and the lack of constraints in free-text rationale generation (Sec. 2.1), it is difficult to establish any priors about $\rho(r_i, \hat{y}_i)$ for arbitrary r_i . To address this gap, the reference rationale upper bound provides a powerful invariance for analyzing free-text rationale quality. Thus, FRAME evaluates Φ by checking that $\Phi(\hat{y}_i) > \Phi(r_i)$ for various r_i (e.g., \hat{r}_i) that are likely to differ in meaning from \hat{y}_i .

Axiom 2: Rationale Perturbation Sensitivity

Rationale r_i should yield high $\rho(r_i, \hat{y}_i)$ if r_i contains the same semantic information as \hat{y}_i , even if r_i and \hat{y}_i do not have the same surface form. Conversely, r_i should yield low $\rho(r_i, \hat{y}_i)$ if r_i differs greatly in meaning from \hat{y}_i . Thus, Φ should be appropriately sensitive when either *equivalent* (does not change r_i 's meaning) or *contrastive* (changes r_i 's meaning) perturbations are applied to r_i . We denote the perturbed rationale as $\Psi(r_i)$, where Ψ is a perturbation function. While Φ should be properly perturbation-sensitive for any rationale r_i , we focus on perturbing \hat{y}_i in this work. This is because the value of $\rho(r_i, \hat{y}_i)$ for arbitrary r_i is unclear, whereas we know $\rho(\hat{y}_i, \hat{y}_i)$ is high. See Sec. A.1 for details about rationale perturbation.

Axiom 3: Robustness to Variation in \mathcal{F}

In general, $\rho(r_i, \hat{y}_i)$ should be independent of whether $\hat{y}_i = \hat{y}_i$ (i.e., \mathcal{F} 's task performance). Since \hat{y}_i always provides full information about itself, it follows that $\Phi(\hat{y}_i)$ should be roughly constant w.r.t. \mathcal{F} 's task performance. Note that arbitrary r_i may not provide such an invariance. For example, if we consider \hat{r}_i (i.e., rationale outputted by \mathcal{F}), then \hat{r}_i 's quality may depend on how \mathcal{F} is trained. Thus, in order to stably compare RLC metrics, we focus on analyzing RLC metrics w.r.t. \hat{y}_i . We vary \mathcal{F} 's performance in the following ways.

First, \mathcal{F} 's task performance can be changed by respectively varying the number of instances for training \mathcal{F} , number of noisy-labeled instances for training \mathcal{F} , and number of parameters in \mathcal{F} . For each version of \mathcal{F} , we compute $\Phi(\hat{y}_i)$. A good Φ should yield similar $\Phi(\hat{y}_i)$ across all \mathcal{F} versions.

Second, we separately compute $\Phi(\hat{y}_i)$ for the subpopulation of instances where \mathcal{F} outputted correct predictions (i.e., $\hat{y}_i = \hat{y}_i$) as well as the subpopulation of instances where \mathcal{F} outputted incorrect predictions (i.e., $\hat{y}_i \neq \hat{y}_i$). A good Φ should

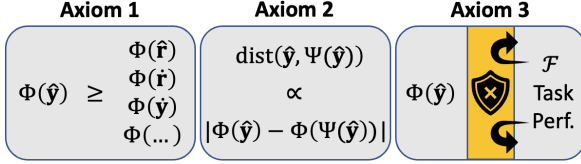


Figure 5: **FRAME Axioms**. FRAME evaluates RLC metrics (Φ) based on three axioms: (1) good Φ should yield highest scores for reference rationales (\hat{y}_i), which maximize RLC by construction; (2) good Φ should be appropriately sensitive to semantic perturbation of rationales ($\Psi(\hat{y}_i)$); and (3) good Φ should be robust to variation in the the task LM’s (\mathcal{F}) task performance.

yield similar $\Phi(\hat{y}_i)$ across both subpopulations.

3.2 FRAME Implementation

Axiom 1: Reference Rationale Upper Bound

For Axiom 1, we want to check if each RLC metric Φ yields the highest scores for \hat{y}_i . First, we report $\Phi(\hat{y}_i)$, where higher scores are better. Second, given a set of non-reference rationales $\mathbf{R}_{\text{NR}} = \{\hat{r}_i, \dot{r}_i, \dot{y}_i\}$, we want to check if Φ yields higher scores for \hat{y}_i than for each $\mathbf{r}_{\text{NR}} \in \mathbf{R}_{\text{NR}}$. To account for scaling differences across different Φ , we want to compare rationales using $\Phi(\hat{y}_i)/\Phi(\mathbf{r}_{\text{NR}})$ instead of $\Phi(\hat{y}_i) - \Phi(\mathbf{r}_{\text{NR}})$. However, $\Phi(\mathbf{r}_{\text{NR}})$ is negative if $\mathbb{1}_{\mathcal{H}}(\hat{y}_i|\mathbf{x}_i, \mathbf{r}_{\text{NR}}) < \mathbb{1}_{\mathcal{G}}(\hat{y}_i|\mathbf{x}_i)$, making $\Phi(\hat{y}_i)/\Phi(\mathbf{r}_{\text{NR}})$ uninformative. Thus, we instead compute accuracy ratio $\mathbb{1}_{\mathcal{H}}(\hat{y}_i|\mathbf{x}_i, \hat{y}_i)/\mathbb{1}_{\mathcal{H}}(\hat{y}_i|\mathbf{x}_i, \mathbf{r}_{\text{NR}})$, since $\mathbb{1}_{\mathcal{G}}(\hat{y}_i|\mathbf{x}_i)$ is constant across all rationales. To aggregate the accuracy ratios, we define the **Mean Accuracy Ratio (MAR)** as the mean $\mathbb{1}_{\mathcal{H}}(\hat{y}_i|\mathbf{x}_i, \hat{y}_i)/\mathbb{1}_{\mathcal{H}}(\hat{y}_i|\mathbf{x}_i, \mathbf{r}_{\text{NR}})$ over all considered non-reference rationales.

Axiom 2: Rationale Perturbation Sensitivity

For Axiom 2, we want to assess if each Φ is appropriately sensitive to semantic perturbation Ψ . Given \hat{y}_i and $\Psi(\hat{y}_i)$, we define the **Absolute Simulatability Difference (ASD)** as $\text{ASD}(a, b) = |\Phi(a) - \Phi(b)|$, with $a = \hat{y}_i$ and $b = \Psi(\hat{y}_i)$. If $\Psi(\hat{y}_i)$ is obtained via equivalent/contrastive perturbation, then lower/higher ASD is better, since \hat{y}_i and $\Psi(\hat{y}_i)$ should be similar/dissimilar in meaning.

Axiom 3: Robustness to Variation in \mathcal{F}

For Axiom 3, we want to assess whether each RLC metric Φ is robust to variation in: (A) the number of instances for training \mathcal{F} (*i.e.*, 100%, 50%, 30%, 10%); (B) number of noisy-labeled instances for training \mathcal{F} (*i.e.*, 0%, 10%, 30%, 50%); (C) number of parameters in \mathcal{F} (*i.e.*, T5-Small, T5-Base, T5-

Large); and (D) \mathcal{F} ’s task performance (*i.e.*, $\hat{y}_i = \dot{y}_i$ vs. $\hat{y}_i \neq \dot{y}_i$). For each variation factor (A)-(C), we compute $\Phi(\hat{y}_i)$ based on each setting within the factor, then compute the mean $\mu(\Phi(\hat{y}_i))$ and standard deviation $\sigma(\Phi(\hat{y}_i))$ over all settings. Generally, lower $\sigma(\Phi(\hat{y}_i))$ indicates higher Φ robustness. However, since $\mu(\Phi(\hat{y}_i))$ can differ greatly across different Φ , we want to account for such scaling differences when comparing $\sigma(\Phi(\hat{y}_i))$. Thus, we instead report the **Sim Coefficient of Variation (SCV)**, defined as $\sigma(\Phi(\hat{y}_i))/\mu(\Phi(\hat{y}_i))$. Lower SCV is better, indicating higher Φ robustness to change in variation settings. For the variation factor (D), we compare $\Phi(\hat{y}_i)$ for \mathcal{F} ’s correctly predicted test instances (*i.e.*, $\Phi_{\hat{y}_i=\dot{y}_i}(\hat{y}_i)$) to $\Phi(\hat{y}_i)$ for \mathcal{F} ’s incorrectly predicted test instances (*i.e.*, $\Phi_{\hat{y}_i \neq \dot{y}_i}(\hat{y}_i)$). To do so, we report $\text{ASD}(a, b)$, with $a = \Phi_{\hat{y}_i=\dot{y}_i}(\hat{y}_i)$ and $b = \Phi_{\hat{y}_i \neq \dot{y}_i}(\hat{y}_i)$.

3.3 RLC Metrics

In this work, we consider four representative RLC metrics, which differ in whether \mathcal{G} and \mathcal{H} are: (A) separate from \mathcal{F} , (B) trained to predict \hat{y}_i , and (C) pretrained on external corpora. The first three (\mathcal{F} -GOLD, $\mathcal{G}\mathcal{H}$ -GOLD, $\mathcal{G}\mathcal{H}$ -PRED) are baselines, while the fourth (NP- $\mathcal{G}\mathcal{H}$ -PRED) is our proposed RLC metric (Fig. 6). Note that prior free-text rationale evaluation works have also studied aspects like label leakage (Hase et al., 2020), input noise robustness (Wiegreffe et al., 2021), and feature importance agreement (Wiegreffe et al., 2021). However, these aspects are orthogonal to the focus of our work (*i.e.*, (A)-(C)), as each existing RLC metric can still be categorized as one of the four we consider. By default, we use T5-Base for \mathcal{F} , \mathcal{G} , and \mathcal{H} . We describe each RLC metric below.

\mathcal{F} -GOLD \mathcal{F} -Gold is a baseline RLC metric introduced by us. Recall \mathcal{F} is first pretrained on external corpora, then finetuned to predict \dot{y}_i . In \mathcal{F} -GOLD, \mathcal{G} is replaced by \mathcal{F} with \mathbf{x}_i as input, while \mathcal{H} is replaced by \mathcal{F} with \mathbf{x}_i and \mathbf{r}_i as input. Thus, \mathcal{G} ’s accuracy in predicting \hat{y}_i is trivially always 100%, which limits \mathcal{F} -Gold’s utility. Unlike other metrics, \mathcal{F} -GOLD does not need to assume \mathcal{F} , \mathcal{G} , and \mathcal{H} are different LMs with similar reasoning processes.

$\mathcal{G}\mathcal{H}$ -GOLD In $\mathcal{G}\mathcal{H}$ -GOLD, \mathcal{G} and \mathcal{H} are first pretrained on external corpora, then finetuned to predict \dot{y}_i . $\mathcal{G}\mathcal{H}$ -GOLD is the RLC metric used in the evaluations proposed by Wiegreffe et al. (2021).

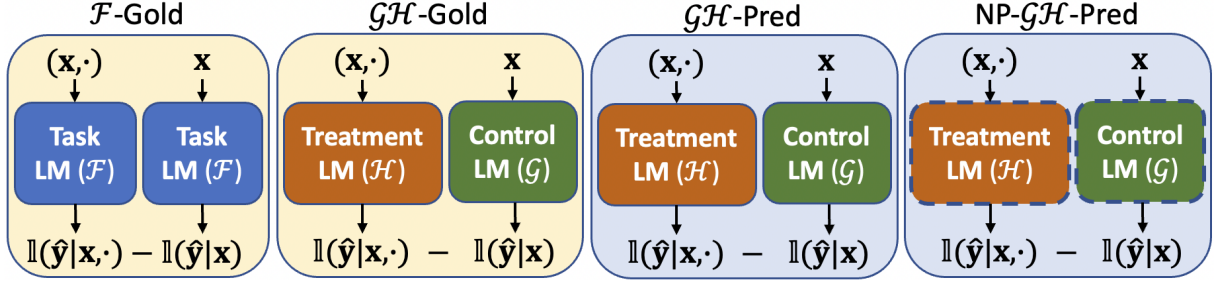


Figure 6: **RLC Metrics.** We consider four RLC metrics (\mathcal{F} -GOLD, \mathcal{GH} -GOLD, \mathcal{GH} -PRED, NP- \mathcal{GH} -PRED) (Sec. 3.3). Metrics with “ \mathcal{F} ” use only \mathcal{F} as the simulator. Metrics with “ \mathcal{GH} ” use \mathcal{G} and \mathcal{H} as simulators. Metrics with “Gold” (yellow background) involve training simulators to predict the gold label \hat{y}_i . Metrics with “Pred” (blue background) involve training simulators to predict \mathcal{F} ’s predicted label \hat{y}_i . NP- \mathcal{GH} -PRED is the only metric without simulator pretraining (dotted lines), which can hurt RLC metrics’ reliability (Sec. 4)

\mathcal{GH} -PRED In \mathcal{GH} -PRED, \mathcal{G} and \mathcal{H} are first pre-trained on external corpora, then finetuned to predict \hat{y}_i . \mathcal{GH} -PRED is very similar in spirit to the RLC metric used in Hase et al. (2020) (Sec. 2).

NP- \mathcal{GH} -PRED NP- \mathcal{GH} -PRED is our proposed RLC metric. Unlike the other metrics, \mathcal{G} and \mathcal{H} are not pre-trained on external corpora. Here, \mathcal{G} and \mathcal{H} are randomly initialized, then trained to predict \hat{y}_i . We hypothesize that this will enable us to better isolate the rationale’s contributions from the pretraining knowledge obtained by pretrained versions of \mathcal{G} and \mathcal{H} . However, not pretraining \mathcal{G} and \mathcal{H} may weaken the assumption that \mathcal{F} , \mathcal{G} , and \mathcal{H} have similar reasoning processes.

4 Experiments

In this section, we present empirical results for FRAME. First, for LM simulators, we investigate FRAME Axioms 1-3 in the context of (automatic) faithfulness evaluation, demonstrating the relative effectiveness of the NP- \mathcal{GH} -PRED RLC metric in measuring rationale quality (Sec. 4.2). Second, for human simulators, we conduct a user study about Axiom 1 to show FRAME’s applicability to (manual) plausibility evaluation, while further establishing NP- \mathcal{GH} -PRED’s effectiveness (Sec. 4.3). For all results, we report the mean and standard deviation over three seeds. In all tables, best performance is highlighted in green, while second-best performance (if applicable) is highlighted in blue.

Normalized Relative Gain (NRG) For each axiom, we would like to summarize all metrics as a single aggregate metric, but this may not be straightforward if different metrics have different scales or different optimal values (*e.g.*, higher is better *vs.* lower is better). Thus, for each axiom,

we summarize all metrics using the Normalized Relative Gain (NRG) metric (Chan et al., 2022), which normalizes all metrics’ scores to values in $[0, 1]$ then outputs the final score by computing the mean of the normalized scores.

4.1 Datasets

We consider closed-set and multi-choice m -class text classification tasks. In closed-set classification (*e.g.*, natural language inference (NLI)), the same m -class label space is used for all instances. In multi-choice classification (*e.g.*, commonsense QA), each instance has a different set of m choices. Following prior works (Hase et al., 2020; Wiegrefe et al., 2021), we experiment with the e-SNLI (Camburu et al., 2018), CoS-E v1.0 (Rajani et al., 2019), and CoS-E v1.1 (Rajani et al., 2019) datasets. e-SNLI is an NLI dataset, while CoS-E v1.0 and CoS-E v1.1 are commonsense QA datasets.

4.2 LM Simulators

Axiom 1: Reference Rationale Upper Bound Table 1 displays results for Axiom 1. NP- \mathcal{GH} -PRED performs best overall, achieving the highest $\Phi(\hat{y}_i)$, MAR, and NRG on all datasets, besides having the second-highest MAR on e-SNLI. None of the other metrics perform consistently well across datasets. For mean NRG over all datasets, NP- \mathcal{GH} -PRED beats the strongest per-dataset baseline by 41.7%, hence best satisfying Axiom 1. This suggests that simulator pretraining worsens RLC metrics’ ability to capture relative rationale-label association across different rationales.

Axiom 2: Rationale Perturbation Sensitivity Table 2 displays results for Axiom 2. NP- \mathcal{GH} -PRED performs best on e-SNLI (w.r.t. Contrastive ASD and NRG) and competitively on CoS-E v1.0

Dataset	RLC Metric	$\Phi(\hat{y}_i)$ (\uparrow)	MAR (\uparrow)	NRG (\uparrow)
e-SNLI	\mathcal{F} -GOLD	-7.27 (± 0.57)	1.45 (± 0.01)	0.50
	\mathcal{GH} -GOLD	-1.70 (± 8.25)	1.01 (± 0.07)	0.04
	\mathcal{GH} -PRED	9.10 (± 0.61)	1.01 (± 0.01)	0.13
	NP- \mathcal{GH} -PRED	54.77 (± 4.27)	1.15 (± 0.01)	0.66
CoS-E v1.0	\mathcal{F} -GOLD	-34.39 (± 1.83)	0.85 (± 0.01)	0.00
	\mathcal{GH} -GOLD	17.93 (± 1.81)	1.33 (± 0.02)	0.65
	\mathcal{GH} -PRED	18.60 (± 0.86)	1.33 (± 0.04)	0.66
	NP- \mathcal{GH} -PRED	23.83 (± 2.17)	2.04 (± 0.09)	1.00
CoS-E v1.11	\mathcal{F} -GOLD	-35.63 (± 1.63)	0.83 (± 0.02)	0.00
	\mathcal{GH} -GOLD	21.16 (± 2.36)	1.47 (± 0.06)	0.70
	\mathcal{GH} -PRED	22.17 (± 1.04)	1.46 (± 0.03)	0.71
	NP- \mathcal{GH} -PRED	23.48 (± 0.60)	2.26 (± 0.09)	1.00

Table 1: **Axiom 1 (LM Simulators)**. We evaluate RLC metrics’ ability to use reference rationale as a faithfulness upper bound. NP- \mathcal{GH} -PRED performs best overall, while none of the RLC metrics are consistently good across all three datasets.

and CoS-E v1.11. However, \mathcal{GH} -GOLD performs best overall, yielding the second-highest NRG on e-SNLI and the highest NRG on CoS-E v1.0 and CoS-E v1.11. We find that the equivalent perturbation property is easier to satisfy, as all metrics except \mathcal{F} -GOLD yield low Equivalent ASD. Meanwhile, the contrastive perturbation property is harder to satisfy, as only \mathcal{GH} -GOLD consistently achieves high Contrastive ASD. These results confirm the limitation of using \mathcal{F} as the simulator, while suggesting that using \hat{y}_i as simulator supervision may help RLC metrics’ semantic sensitivity.

Dataset	RLC Metric	Equivalent	Contrastive	All
		ASD (\downarrow)	ASD (\uparrow)	NRG (\uparrow)
e-SNLI	\mathcal{F} -GOLD	11.80 (± 0.60)	12.50 (± 0.44)	0.10
	\mathcal{GH} -GOLD	6.10 (± 7.96)	40.53 (± 7.03)	0.74
	\mathcal{GH} -PRED	0.00 (± 0.00)	5.23 (± 1.02)	0.50
	NP- \mathcal{GH} -PRED	0.07 (± 0.12)	40.83 (± 2.63)	1.00
CoS-E v1.0	\mathcal{F} -GOLD	5.61 (± 2.00)	26.91 (± 2.37)	0.09
	\mathcal{GH} -GOLD	0.67 (± 0.40)	83.09 (± 13.16)	0.94
	\mathcal{GH} -PRED	0.00 (± 0.00)	15.09 (± 4.29)	0.50
	NP- \mathcal{GH} -PRED	0.74 (± 0.76)	26.21 (± 2.79)	0.52
CoS-E v1.11	\mathcal{F} -GOLD	4.04 (± 0.31)	26.13 (± 2.15)	0.04
	\mathcal{GH} -GOLD	0.96 (± 1.65)	84.14 (± 21.59)	0.93
	\mathcal{GH} -PRED	0.00 (± 0.00)	21.57 (± 1.04)	0.50
	NP- \mathcal{GH} -PRED	1.42 (± 0.48)	25.55 (± 0.99)	0.36

Table 2: **Axiom 2 (LM Simulators)**. We evaluate RLC metrics’ sensitivity to semantic perturbation of rationales. We find that \mathcal{GH} -GOLD performs best overall, while NP- \mathcal{GH} -PRED also consistently performs well across all three datasets.

Axiom 3: Robustness to Variation in \mathcal{F} Table 3 and Fig. 7-9 display results for Axiom 3. In Table 3, NP- \mathcal{GH} -PRED greatly outperforms all baselines all meta-metrics, yielding a perfect NRG of 1.00 on all datasets. None of the other metrics perform consistently well across datasets. Similarly, in Fig.

7-9, NP- \mathcal{GH} -PRED yields much flatter curves than other RLC metrics do, indicating its relative robustness to changes in \mathcal{F} ’s number of train instances (Fig. 7), number of noisy train instances (Fig. 8), and task performance (Fig. 9). For mean NRG over all datasets, NP- \mathcal{GH} -PRED beats the strongest per-dataset baselines by 42.9%, hence best satisfying Axiom 3. This suggests that simulator pretraining hurts RLC metrics’ ability to disentangle rationale-label association from \mathcal{F} ’s task performance.

Dataset	RLC Metric	% Train	% Noisy Train	Capacity	Subpop.	All
		SCV (\downarrow)	SCV (\downarrow)	SCV (\downarrow)	ASD (\downarrow)	NRG (\uparrow)
e-SNLI	\mathcal{F} -GOLD	0.27 (± 0.06)	0.34 (± 0.13)	0.81 (± 0.18)	6.81 (± 1.51)	0.27
	\mathcal{GH} -GOLD	0.14 (± 0.26)	0.71 (± 0.26)	0.65 (± 0.21)	20.18 (± 4.20)	0.26
	\mathcal{GH} -PRED	0.11 (± 0.02)	0.21 (± 0.02)	0.16 (± 0.04)	32.97 (± 3.36)	0.69
	NP- \mathcal{GH} -PRED	0.02 (± 0.01)	0.03 (± 0.02)	0.04 (± 0.00)	1.85 (± 1.12)	1.00
CoS-E v1.0	\mathcal{F} -GOLD	0.13 (± 0.11)	0.21 (± 0.12)	0.55 (± 0.05)	23.41 (± 1.79)	0.71
	\mathcal{GH} -GOLD	0.25 (± 0.13)	0.40 (± 0.22)	0.43 (± 0.18)	27.56 (± 0.87)	0.15
	\mathcal{GH} -PRED	0.32 (± 0.19)	0.22 (± 0.04)	0.08 (± 0.04)	23.20 (± 4.39)	0.30
	NP- \mathcal{GH} -PRED	0.08 (± 0.02)	0.10 (± 0.00)	0.05 (± 0.02)	5.37 (± 4.51)	1.00
CoS-E v1.11	\mathcal{F} -GOLD	0.14 (± 0.03)	0.16 (± 0.07)	0.63 (± 0.08)	25.48 (± 1.77)	0.57
	\mathcal{GH} -GOLD	0.23 (± 0.05)	0.32 (± 0.09)	0.40 (± 0.05)	22.61 (± 1.87)	0.00
	\mathcal{GH} -PRED	0.05 (± 0.02)	0.22 (± 0.02)	0.32 (± 0.01)	25.47 (± 1.22)	0.70
	NP- \mathcal{GH} -PRED	0.05 (± 0.01)	0.07 (± 0.01)	0.09 (± 0.02)	6.28 (± 2.05)	1.00

Table 3: **Axiom 3 (LM Simulators)**. We evaluate RLC metrics’ robustness to four types of variation in \mathcal{F} . Here, NP- \mathcal{GH} -PRED greatly outperforms other RLC metrics across all datasets.

4.3 Human Simulators

Beyond faithfulness (Sec. 4.2), we want to show that FRAME can also be used to evaluate rationale plausibility. Whereas faithfulness evaluation can be automated due to its use of LM simulators, plausibility evaluation requires significant manual effort from human simulators. Since Axioms 2-3 have many more experiment settings than Axiom 1, they require much more manual effort for plausibility evaluation. Thus, as a proof of concept, we conduct a plausibility user study based on Axiom 1, using a subset of the four RLC metrics.

Our goal is to verify that our Axiom 1 conclusions for faithfulness (Table 1) also hold for plausibility. This means we must reframe the RLC metrics w.r.t. human simulators, which requires three more assumptions. First, we assume human simulators are pretrained, since they should possess general language understanding abilities and world knowledge. Second, we assume human simulators already know how to solve the given task (*i.e.*, already finetuned to predict \hat{y}_i), using either \mathbf{x}_i or $(\mathbf{x}_i, \mathbf{r}_i)$ as input. Third, we assume human simulators can learn patterns from few training examples.

Based on these assumptions, we compare \mathcal{GH} -GOLD and NP- \mathcal{GH} -PRED. For \mathcal{GH} -GOLD, given the assumed pretraining/finetuning, we simply compute Φ without further training. However, for NP-

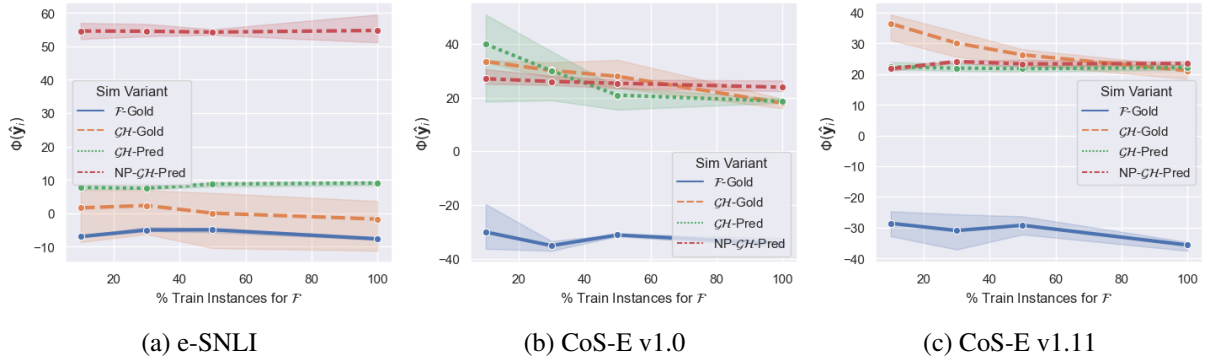


Figure 7: **Axiom 3 (LM Simulators): % Train Instances for \mathcal{F} vs. $\Phi(\hat{y}_i)$.** Flatter curves mean greater robustness to change in \mathcal{F} task performance, by varying the percentage of train instances for \mathcal{F} .

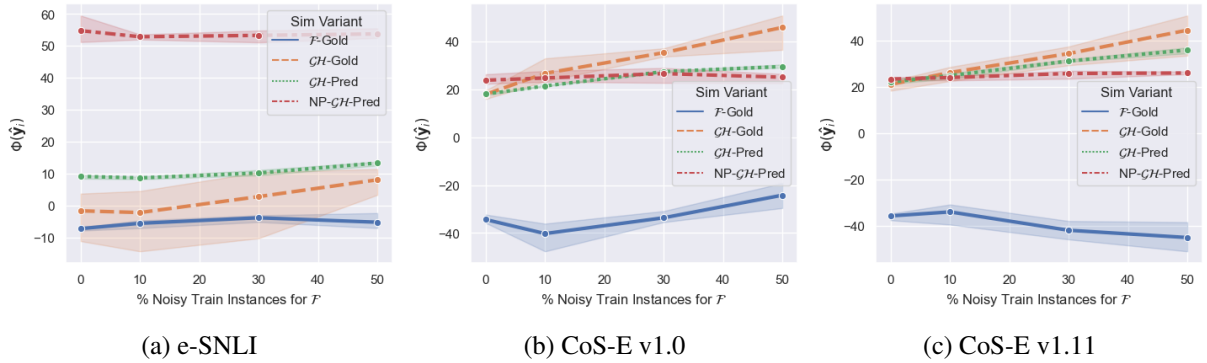


Figure 8: **Axiom 3 (LM Simulators): % Noisy Train Instances for \mathcal{F} vs. $\Phi(\hat{y}_i)$.** Flatter curves mean greater robustness to change in \mathcal{F} task performance, by varying the percentage of noisy train instances for \mathcal{F} .

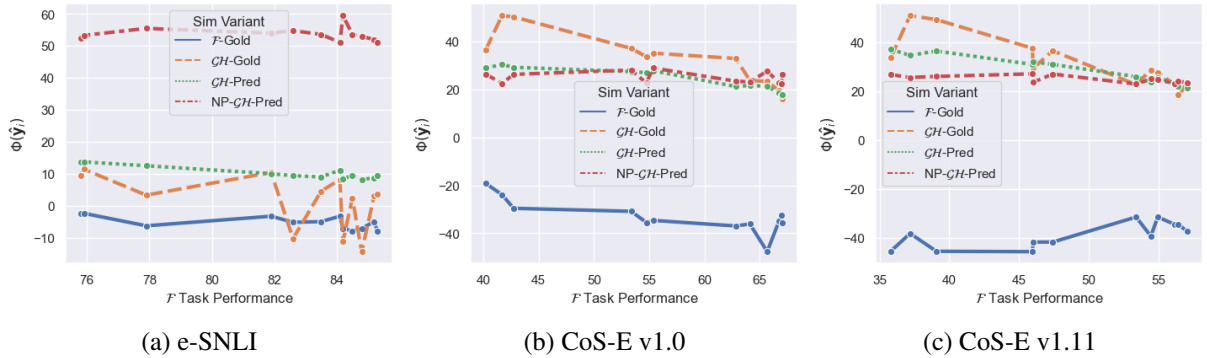


Figure 9: **Axiom 3 (LM Simulators): \mathcal{F} Task Performance vs. $\Phi(\hat{y}_i)$.** Flatter curves mean greater robustness to change in \mathcal{F} task performance, by varying the percentage of noisy train instances for \mathcal{F} . Unlike in Fig. 8, we directly plot $\Phi(\hat{y}_i)$ as a function of \mathcal{F} task performance here.

\mathcal{GH} -PRED, we need to disable pretraining and train the simulator to predict \hat{y}_i . To simulate the disabling of pretraining, we encrypt every character in the dataset using a Caesar cipher (Savarese and Hart, 1999) with right shift 1 (e.g., *hello* \rightarrow *ifmmp*). Each encrypted instance still encodes the same information as before, but encryption hinders human simulators from leveraging their language priors. Thus, human simulators must rely on patterns

learned while they are newly trained to predict \hat{y}_i .

We uniformly sample 50 test instances from CoS-E v1.0, then ask five human annotators to serve as simulators for Axiom 1, as both \mathcal{GH} -GOLD and NP- \mathcal{GH} -PRED. Besides computing $\Phi(\hat{y}_i)$ and MAR, we also ask annotators to rate their confidence for each sim accuracy term (i.e., $\mathbb{1}_{\mathcal{G}}(\hat{y}_i|\mathbf{x}_i)$, $\mathbb{1}_{\mathcal{H}}(\hat{y}_i|\mathbf{x}_i, \hat{\mathbf{r}}_i)$, $\mathbb{1}_{\mathcal{H}}(\hat{y}_i|\mathbf{x}_i, \hat{\mathbf{r}}_i)$, $\mathbb{1}_{\mathcal{H}}(\hat{y}_i|\mathbf{x}_i, \hat{y}_i)$, $\mathbb{1}_{\mathcal{H}}(\hat{y}_i|\mathbf{x}_i, \hat{y}_i)$), on a 4-point Likert

RLC Metric	Sim-Based Scores		Confidence				
	$\Phi(\hat{y}_i)$ (\uparrow)	MAR (\uparrow)	$\mathbb{1}_{\mathcal{G}}(\mathbf{x})$ (\downarrow)	$\mathbb{1}_{\mathcal{H}}(\mathbf{x}, \hat{\mathbf{r}})$ (\downarrow)	$\mathbb{1}_{\mathcal{H}}(\mathbf{x}, \hat{\mathbf{r}})$ (\downarrow)	$\mathbb{1}_{\mathcal{H}}(\mathbf{x}, \hat{y})$ (\downarrow)	$\mathbb{1}_{\mathcal{H}}(\mathbf{x}, \hat{y})$ (\uparrow)
\mathcal{GH} -GOLD	51.60 (± 28.00)	2.03 (± 0.53)	2.94 (± 0.37)	3.06 (± 0.47)	3.47 (± 0.35)	3.72 (± 0.36)	3.41 (± 0.66)
NP- \mathcal{GH} -PRED	71.60 (± 7.65)	3.18 (± 0.60)	1.13 (± 0.25)	1.82 (± 0.66)	1.76 (± 0.73)	2.84 (± 1.16)	3.44 (± 0.86)

Table 4: **Axiom 1 (Human Simulators)**. We conduct a user study to investigate FRAME’s applicability to plausibility evaluation (*i.e.*, using human simulators) w.r.t. Axiom 1. Our results mirror those for faithfulness evaluation, with NP- \mathcal{GH} -PRED consistently outperforming \mathcal{GH} -GOLD.

scale (*i.e.*, higher rating \rightarrow higher confidence).

Table 4 displays the user study results. On $\Phi(\hat{y}_i)$ and MAR, NP- \mathcal{GH} -PRED greatly outperforms \mathcal{GH} -GOLD, corroborating the results in Table 1. Specifically, across $\Phi(\hat{y}_i)$ and MAR, NP- \mathcal{GH} -PRED yields a 47.7% mean improvement over \mathcal{GH} -GOLD, while also having much lower standard deviation on $\Phi(\hat{y}_i)$. Furthermore, NP- \mathcal{GH} -PRED yields much higher confidence than \mathcal{GH} -GOLD for $\mathbb{1}_{\mathcal{H}}(\hat{y}_i|\mathbf{x}, \hat{y})$, relative to the other four settings. In other words, for NP- \mathcal{GH} -PRED, annotators not only yield higher $\Phi(\hat{y})$, but also do so more confidently. These results demonstrate FRAME’s applicability to plausibility evaluation as well as NP- \mathcal{GH} -PRED’s effectiveness as a plausibility metric.

5 Related Work

Extractive Rationale Evaluation Most rationale evaluation works focus on extractive rationales. Existing faithfulness metrics for extractive rationales are based on rationale-label association, either via heuristic functions (DeYoung et al., 2019; Shrikumar et al., 2017; Sanyal and Ren, 2021; Hase and Bansal, 2020) or model retraining (Hooker et al., 2018; Pruthi et al., 2020). For example, Pruthi et al. (2020) measures the faithfulness of a teacher LM’s rationales as how well a student LM can predict the teacher’s predicted labels when regularized using those rationales. Meanwhile, existing plausibility metrics for extractive rationales are based on rationale-label association (Hase and Bansal, 2020; Strout et al., 2019; Chan et al., 2022) or gold rationale similarity (DeYoung et al., 2019; Chan et al., 2022). However, evaluating plausibility via gold rationale similarity is noisy because gold rationales are defined w.r.t. the gold label, not the task LM’s predicted label (Chan et al., 2022).

Like Pruthi et al. (2020), our NP- \mathcal{GH} -PRED metric trains a student (simulator) LM to predict a teacher (task) LM’s labels, though we focus on free-text rationales and simply append the rationale to the student’s input. We do not apply FRAME to extractive rationales, since it is not straightforward

to construct extractive reference rationales.

Free-Text Rationale Evaluation Few works consider free-text rationale evaluation. Like for extractive rationales, free-text rationale faithfulness is evaluated via rationale-label association, while Existing faithfulness metrics for free-text rationales are based on rationale-label association and implemented via sim (Sec. 2.2) (Hase et al., 2020; Wiegrefe et al., 2021), which evaluates rationales w.r.t. its predictiveness of the task LM’s labels (Doshi-Velez and Kim, 2017). Hase et al. (2020) proposes LAS, a sim-based metric that controls for label leakage by the rationale. Wiegrefe et al. (2021) proposes two sim-based metrics: RE measures sim w.r.t. input noise robustness, while FIA measures sim w.r.t. feature importance agreement. Existing plausibility metrics for free-text rationales can be based on sim (Hase et al., 2020) or gold rationale similarity (Narang et al., 2020).

Crucially, existing RLC metrics pretrain the simulator LM on external corpora, which makes it difficult to isolate the rationale’s contribution from the simulator LM’s pretraining knowledge. Using FRAME, we show this results in oversensitivity to the task LM’s task performance and that our non-pretrained NP- \mathcal{GH} -PRED performs better on FRAME meta-metrics. Our contributions are orthogonal to those in LAS, RE, and FIA, as NP- \mathcal{GH} -PRED can be applied to all of these metrics.

6 Conclusion

In this paper, we showed that using non-pretrained simulators (*i.e.*, NP- \mathcal{GH} -PRED) for RLC-based rationale evaluation can better satisfy the desired FRAME properties than using pretrained simulators. While these results demonstrate the relative effectiveness of the NP- \mathcal{GH} -PRED RLC metric, they also reveal the inherent limitations of using sim to evaluate rationale quality. First, although reference rationales maximize RLC, they generally provide very limited information about an LM’s or human’s reasoning process. This suggests that

RLC alone cannot sufficiently capture faithfulness or plausibility. Second, sim requires that the task LM and simulator are distinct, or else the simulator will trivially achieve perfect accuracy when using the original task input. As a result, sim-based faithfulness evaluation calls for the strong assumption that the simulator’s reasoning process is representative of the task LM’s. As RLC metrics can vary w.r.t. how the simulator is trained, it is unclear which simulator training procedures are acceptable for justifying the above assumption. Though RLC can provide useful signal about rationale quality, these limitations suggest that future work on rationale evaluation should move beyond RLC.

References

- Emily M Bender, Timnit Gebru, Angelina McMillan-Major, and Shmargaret Shmitchell. 2021. On the dangers of stochastic parrots: Can language models be too big? . In *Proceedings of the 2021 ACM Conference on Fairness, Accountability, and Transparency*, pages 610–623.
- Oana-Maria Camburu, Tim Rocktäschel, Thomas Lukasiewicz, and Phil Blunsom. 2018. e-snli: Natural language inference with natural language explanations. *arXiv preprint arXiv:1812.01193*.
- Aaron Chan, Maziar Sanjabi, Lambert Mathias, Liang Tan, Shaoliang Nie, Xiaochang Peng, Xiang Ren, and Hamed Firooz. 2022. Unirex: A unified learning framework for language model rationale extraction. *arXiv preprint arXiv:2112.08802*.
- Misha Denil, Alban Demiraj, and Nando De Freitas. 2014. Extraction of salient sentences from labelled documents. *arXiv preprint arXiv:1412.6815*.
- Jacob Devlin, Ming-Wei Chang, Kenton Lee, and Kristina Toutanova. 2018. Bert: Pre-training of deep bidirectional transformers for language understanding. *arXiv preprint arXiv:1810.04805*.
- Jay DeYoung, Sarthak Jain, Nazneen Fatema Rajani, Eric Lehman, Caiming Xiong, Richard Socher, and Byron C Wallace. 2019. Eraser: A benchmark to evaluate rationalized nlp models. *arXiv preprint arXiv:1911.03429*.
- Virginie Do, Oana-Maria Camburu, Zeynep Akata, and Thomas Lukasiewicz. 2020. e-snli-ve: Corrected visual-textual entailment with natural language explanations. *arXiv preprint arXiv:2004.03744*.
- Finale Doshi-Velez and Been Kim. 2017. Towards a rigorous science of interpretable machine learning. *arXiv preprint arXiv:1702.08608*.
- Peter Hase and Mohit Bansal. 2020. Evaluating explainable ai: Which algorithmic explanations help users predict model behavior? In *Proceedings of the 58th Annual Meeting of the Association for Computational Linguistics*, pages 5540–5552.
- Peter Hase, Shiyue Zhang, Harry Xie, and Mohit Bansal. 2020. Leakage-adjusted simulatability: Can models generate non-trivial explanations of their behavior in natural language? In *Findings of the Association for Computational Linguistics: EMNLP 2020*, pages 4351–4367.
- Sara Hooker, Dumitru Erhan, Pieter-Jan Kindermans, and Been Kim. 2018. A benchmark for interpretability methods in deep neural networks. *arXiv preprint arXiv:1806.10758*.
- Alon Jacovi and Yoav Goldberg. 2020. Towards faithfully interpretable nlp systems: How should we define and evaluate faithfulness? *arXiv preprint arXiv:2004.03685*.
- Ziwei Ji, Nayeon Lee, Rita Frieske, Tiezheng Yu, Dan Su, Yan Xu, Etsuko Ishii, Yejin Bang, Andrea Madotto, and Pascale Fung. 2022. Survey of hallucination in natural language generation. *arXiv preprint arXiv:2202.03629*.
- Sawan Kumar and Partha Talukdar. 2020. Nile: Natural language inference with faithful natural language explanations. *arXiv preprint arXiv:2005.12116*.
- Kushal Lakhotia, Bhargavi Paranjape, Asish Ghoshal, Wen-tau Yih, Yashar Mehdad, and Srinivasan Iyer. 2020. Fid-ex: Improving sequence-to-sequence models for extractive rationale generation. *arXiv preprint arXiv:2012.15482*.
- Zachary C Lipton. 2018. The mythos of model interpretability: In machine learning, the concept of interpretability is both important and slippery. *Queue*, 16(3):31–57.

- Hui Liu, Qingyu Yin, and William Yang Wang. 2018. Towards explainable nlp: A generative explanation framework for text classification. *arXiv preprint arXiv:1811.00196*.
- Yinhan Liu, Myle Ott, Naman Goyal, Jingfei Du, Mandar Joshi, Danqi Chen, Omer Levy, Mike Lewis, Luke Zettlemoyer, and Veselin Stoyanov. 2019. Roberta: A robustly optimized bert pretraining approach. *arXiv preprint arXiv:1907.11692*.
- Sharan Narang, Colin Raffel, Katherine Lee, Adam Roberts, Noah Fiedel, and Karishma Malkan. 2020. Wt5?! training text-to-text models to explain their predictions. *arXiv preprint arXiv:2004.14546*.
- Dong Huk Park, Lisa Anne Hendricks, Zeynep Akata, Anna Rohrbach, Bernt Schiele, Trevor Darrell, and Marcus Rohrbach. 2018. Multimodal explanations: Justifying decisions and pointing to the evidence. In *Proceedings of the IEEE Conference on Computer Vision and Pattern Recognition*, pages 8779–8788.
- Danish Pruthi, Bhuwan Dhingra, Livio Baldini Soares, Michael Collins, Zachary C Lipton, Graham Neubig, and William W Cohen. 2020. Evaluating explanations: How much do explanations from the teacher aid students? *arXiv preprint arXiv:2012.00893*.
- Colin Raffel, Noam Shazeer, Adam Roberts, Katherine Lee, Sharan Narang, Michael Matena, Yanqi Zhou, Wei Li, and Peter J Liu. 2019. Exploring the limits of transfer learning with a unified text-to-text transformer. *arXiv preprint arXiv:1910.10683*.
- Nazneen Fatema Rajani, Bryan McCann, Caiming Xiong, and Richard Socher. 2019. Explain yourself! leveraging language models for commonsense reasoning. *arXiv preprint arXiv:1906.02361*.
- Cynthia Rudin. 2019. Stop explaining black box machine learning models for high stakes decisions and use interpretable models instead. *Nature Machine Intelligence*, 1(5):206–215.
- Soumya Sanyal and Xiang Ren. 2021. Discretized integrated gradients for explaining language models. *arXiv preprint arXiv:2108.13654*.
- Chris Savarese and Brian Hart. 1999. The caesar cipher. *Historical Cryptography Web Site*.
- Avanti Shrikumar, Peyton Greenside, and Anshul Kundaje. 2017. Learning important features through propagating activation differences. In *International Conference on Machine Learning*, pages 3145–3153. PMLR.
- Julia Strout, Ye Zhang, and Raymond J Mooney. 2019. Do human rationales improve machine explanations? *arXiv preprint arXiv:1905.13714*.
- Mukund Sundararajan, Ankur Taly, and Qiqi Yan. 2017. Axiomatic attribution for deep networks. In *International Conference on Machine Learning*, pages 3319–3328. PMLR.
- Sarah Wiegrefe, Ana Marasović, and Noah A Smith. 2021. Measuring association between labels and free-text rationales. In *Proceedings of the 2021 Conference on Empirical Methods in Natural Language Processing*, pages 10266–10284.
- Jialin Wu and Raymond J Mooney. 2018. Faithful multimodal explanation for visual question answering. *arXiv preprint arXiv:1809.02805*.

A Appendix

A.1 Rationale Perturbation

Equivalent Perturbation Let Ψ_e be an equivalent perturbation function which modifies \mathbf{r}_i 's surface form without changing \mathbf{r}_i 's semantic content. That is, \mathbf{r}_i and $\Psi_e(\mathbf{r}_i)$ have different surface forms but share the same meaning. In this paper, we consider the closed-set (e-SNLI) and multi-choice (CoS-E v1.0, CoS-E v1.11) text classification tasks. Each task requires a different form of Ψ_e .

For closed-set classification, \mathbf{r}_i is generally a single-word label (e.g., "entailment"), hence yielding a single-word reference rationale. Such single-word rationales are not representative of free-text rationales, which are motivated as being accessible natural language sentences. Here, we design Ψ_e to construct $\Psi_e(\mathbf{r}_i)$ by paraphrasing \mathbf{r}_i as a natural language sentence. For each class c_j in the m -class label space $C = \{c_j\}_{j=1}^m$, we manually write a set of k paraphrase sentences S_j , based only on c_j (i.e., not on \mathbf{x}_i). Given task instance i and \mathcal{F} 's predicted label y_i , suppose $y_i = c_j$ for some j . After setting $\mathbf{r}_i = y_i$, we obtain $\Psi_e(\mathbf{r}_i)$ by randomly sampling a paraphrase sentence s from S_j then setting $\Psi_e(\mathbf{r}_i) = s$, e.g., if $\mathbf{r}_i = \text{"contradiction"}$, and $s = \text{"The hypothesis conflicts with the premise."}$, the resulting $\Psi_e(\mathbf{r}_i)$ would be "The hypothesis conflicts with the premise."

For multi-choice classification, \mathbf{r}_i is generally a multi-word choice (e.g., "have fun in the park"), hence yielding a multi-word reference rationale \mathbf{r}_i . Since each instance has a different set of choices, it is not feasible to manually write paraphrase sentences specifically for every choice across all instances in the dataset. Instead, we design Ψ_e to perturb \mathbf{r}_i by inserting a generic supporting sentence in front of \mathbf{r}_i . First, we manually write a set, S , of k sentences, each generically expressing affirmation for a subsequent rationale. Note that these sentences are written independently of any particular task input, label, or rationale. Then, for each instance i , we randomly sample one sentence s from S to insert before \mathbf{r}_i . For example, if $\mathbf{r}_i = \text{"I am a rationale."}$, and $s = \text{"The following rationale is faithful: "}$, then the resulting $\Psi_e(\mathbf{r}_i)$ would be "The following rationale is faithful: I am a rationale."

For both tasks, we can see that $\Psi_e(\mathbf{r}_i)$ is constructed in a way that does not change the meaning of \mathbf{r}_i . Therefore, in both cases, a good Φ should yield a low value of $|\Phi(\mathbf{r}_i) - \Phi(\Psi_e(\mathbf{r}_i))|$.

Contrastive Perturbation Let Ψ_c be an contrastive perturbation function which modifies \mathbf{r}_i 's surface form while also significantly changing \mathbf{r}_i 's semantic content. That is, \mathbf{r}_i and $\Psi_c(\mathbf{r}_i)$ should have dissimilar surface forms and meaning.

For both closed-set and multi-choice classification, we can construct $\Psi_c(\mathbf{r}_i)$ in the same way. For each instance i , y_i is one of m classes, so we obtain $\Psi_c(\mathbf{r}_i)$ by randomly sampling one of the other $m - 1$ classes to replace \mathbf{r}_i with. We can see that $\Psi_c(\mathbf{r}_i)$ is constructed in a way that fundamentally changes the meaning of \mathbf{r}_i . Therefore, a good Φ should yield a high value of $|\Phi(\mathbf{r}_i) - \Phi(\Psi_c(\mathbf{r}_i))|$.